

This work has been submitted to the IEEE for possible publication. Copyright may be transferred without notice, after which this version may no longer be accessible.



# Head and eye egocentric gesture recognition for human-robot interaction using eyewear cameras \*

Javier Marina-Miranda<sup>1</sup> and V. Javier Traver<sup>2</sup>

<sup>1</sup>Universitat Jaume I, E12071-Castellón, Spain

<sup>2</sup>Institute of New Imaging Technologies, Universitat Jaume I  
E12071-Castellón, Spain  
vtraver@uji.es

## Abstract

Non-verbal communication plays a particularly important role in a wide range of scenarios in Human-Robot Interaction (HRI). Accordingly, this work addresses the problem of human gesture recognition. In particular, we focus on head and eye gestures, and adopt an egocentric (first-person) perspective using eyewear cameras. We argue that this egocentric view offers a number of conceptual and technical benefits over scene- or robot-centric perspectives.

A motion-based recognition approach is proposed, which operates at two temporal granularities. Locally, frame-to-frame homographies are estimated with a convolutional neural network (CNN). The output of this CNN is input to a long short-term memory (LSTM) to capture longer-term temporal visual relationships, which are relevant to characterize gestures.

Regarding the configuration of the network architecture, one particularly interesting finding is that using the output of an internal layer of the homography CNN increases the recognition rate with respect to using the homography matrix itself. While this work focuses on action recognition, and no robot or user study has been conducted yet, the system has been designed to meet real-time constraints. The encouraging results suggest that the proposed egocentric perspective is viable, and this proof-of-concept work provides novel and useful contributions to the exciting area of HRI.

## 1 INTRODUCTION

With the advances in Social Robotics, Human-Robot Interaction (HRI) is an increasingly important area of research. Much work has been conducted on the *robot* side of the interaction so as to generate gaze and body motions which are expressive [1], natural and effective for interaction [16] and collaborations [23, 25], and correspond well to human speech [20, 9]. However, given the importance of non-verbal cues in communication, a successful interaction requires the proper analysis of *human* action [11] as well. While head and eye-based gestures have been investigated in the broader context of human-computer interaction [19, 5, 27, 26, 8], less efforts have arguably

been devoted in the HRI domain, for instance, to assist and improve human-robot task performance [2, 7].

In this work, the use of visual-based egocentric perspective for head and eye gesture recognition in the context of HRI is proposed. We argue that the first-person view (FPV) offers benefits over a third-person view (TPV), as follows: (1) the hard problem of localizing and segmenting human body parts is naturally circumvented; (2) no external (scene or robot) cameras are required; (3) no need that cameras point in specific direction, so the robot might respond to user gestures even if it is not facing the person or is unaware of their presence; (4) the robot does not need to be nearby (it can be in another room in a building or even far away); (5) multiple robots can potentially be interacted with using a single eyewear device. There are certainly also some drawbacks such as that the eyewear devices may be uncomfortable to wear, and they might be less cost-effective if multiple persons have to interact with a shared robot. Occlusions may affect both FPV and TPV, although differently, so a redundant system with both types of cameras can perform synergistically and overcome this limitation.

Despite the potential advantages of the egocentric-based head and eye gesture recognition, this problem has been scarcely addressed in HRI. Exceptions include a system to request and guide a robot to find some object [29], helping navigation to wheelchair users with limited hand mobility [14], or predicting user intention from gaze in grasping tasks [13] and hand-held robots [24]. Most of these works have in common that they seek to assist disabled people. While these are very important target users to consider, we believe the egocentric perspective can benefit a larger general population, in particular when it comes to interacting with robots in our daily-life environments.

To address the problem of egocentric head and eye gesture recognition, we propose a motion-based, computer vision system which operates at two temporal levels of the incoming egocentric visual streams. First, frame-to-frame motions are analyzed with a convolutional neural network (CNN) for homography estimation. The output of this network is used as input to a long short-term memory (LSTM) so as to capture longer-range temporal dependencies required to characterize gestures. LSTMs have recently been proposed in the context of human action recognition, for example using 3D skeleton data encoding parts and joints of the human body [15, 22, 3], or in multimodal approaches [10].

The contributions of this work are: (1) An egocentric per-

---

\*Work supported by project UJI-B2018-44 from *Pla de promoció de la investigació de la Universitat Jaume I, Castelló, Spain*. The financial support for the research network with code RED2018-102511-T, from *Ministerio de Ciencia, Innovación y Universidades*, is acknowledged.



Table 1: Proposed IU catalog. The IUs in bold are followed by the identifier used in this paper. The type of IU and involved eyewear images are also given

Interaction unit	Type	Image(s)
<b>Neutral</b> (Neutral)	-	-
<b>Come here</b> (ComeHere)	Dir	W
Go away	Dir	TBD
Stop	Dir	TBD
Listen! Look! Hey!	Dir	TBD
<b>Head nod</b> (NoddingHead)	Rep	W, E
Partial nodding	Rep	W, E
<b>Head shake</b> (ShakingHead)	Rep	W, E
<b>Positive surprise</b> (Surprise)	Exp	W, E
Negative surprise	Exp	TBD
<b>Maybe</b> (Maybe)	Rep	W

spective for head and eye gesture recognition for HRI. (2) The exploration of an homography estimation network and its joint use with LSTMs. (3) Design decisions and experimental work that provide additional insights for interested practitioners to develop similar systems.

## 2 METHODOLOGY

To address the problem of head and eye gesture recognition, an eyewear device with a world camera (W) and one or two eye cameras (E) is required.

### 2.1 Gestures

Some studies propose generic gestures for deictic hand gestures [4], grasp types [6], or combining hand gestures and language in the context of HRI [17], but nothing was found regarding head and eye gestures, specifically for the context of HRI, that could guide our work.

Therefore, the following criteria for hand and eye gestures were considered: (1) oriented to social robots; (2) general (not application-dependent); (3) universal (easily understandable by users); (4) natural (avoiding gestures which are hard to perform or memorize); and (5) supportive (to express common communication needs).

With these criteria in mind, an initial catalog of interaction units (IUs) was proposed (Table 1). The IUs have been classified according to the taxonomy of illocutionary acts [21], which includes *representatives* (Rep) for assertions, *directives* (Dir) for requests or commands, *commissives* for promises, *expressives* (Exp) for psychological states, and *declarations*. Although this proposal is not definitive and this work only explores a subset of it (the boldfaced IUs, illustrated in videos in the folder ‘gestures’ of Supplementary material), we believe it is a good starting point that can guide further work.

### 2.2 Network architecture and training

For gesture recognition, we propose a motion-based approach which processes image sequences at two temporal levels (Figure 1). First, to analyze global motion between two consecutive

video frames, we explore a convolutional network for homography estimation [28], which we refer to as CAUDHE (Content-Aware Unsupervised Deep Homography Estimation). Two key features of this recently proposed network are (1) its unsupervised nature, which facilitates training since no true homography values are required for each input frame pair, and (2) its robustness to independently moving objects since the object regions are masked out through an outlier rejector. CAUDHE addresses some limitations of previous works such as an unsupervised approach [18], whose loss function operates on intensity values rather than on feature space. Second, to capture long-term visual relationships, the output of CAUDHE is used as input to a long short-term memory (LSTM). For the size of the output of the LSTM, values  $\{16, 32, \dots, 512\}$  were tested, and 128 was chosen as a good balance between model accuracy and computational cost. A single-layer LSTM was chosen since no benefit was observed with more layers (2, 4 and 8). Including a batch normalization (BN) layer previous to the input to the LSTM was observed to result in slightly lower *maximum* test accuracy over a set of training runs. However, on average, including this BN layer results in more stable training, quicker convergence, and better *average* accuracy, which we found generally preferable. After the LSTM, a classification module of a fully connected (FC) layer of  $N$  units is used, with  $N$  the number of IUs considered.

For training, the available pretrained CAUDHE’s weights<sup>1</sup> were used, and the weights of the LSTM and the FC layer were supervisedly learned using the true IU labels, with the negative log likelihood as the loss function. Figure 1 illustrates the complete proposed model, which includes two CAUDHE instances, for the the head and the eye images, respectively. The outputs of these two CNNs are concatenated and input to the LSTM network, as reasoned before.

For the actual training of the rest of the model (the sequence analysis and IU classification parts in Figure 1), the precomputed features ( $\mathbf{m}_t$ ) from the training videos were split into snippets of length  $S = 40$  and overlap  $O = 30$ . Batches of  $M = 32$  snippets were used for training speedup, better performance of the BN layer, and faster convergence.

### 2.3 Practical considerations

Two important design factors for the system to perform efficiently and effectively are the frame rate and the image sizes, since they play important roles in different aspects, and a careful design and proper tradeoff is called for. Since CAUDHE assumes a small baseline ( $B$ ) in the input frame pairs, the higher the frame rate ( $f$ ), the more likely this constraint will be satisfied. On the other hand, the world camera of the eyewear device can operate at several spatial resolutions (from 1080p Full HD to QVGA), but the highest frame rates are only selectable with lower resolutions of these world images. Furthermore, higher quality images have a notable GPU memory footprint, often exceeding the available resources. Therefore, since frames will be later resized, it makes little sense to acquire frames at high spatial resolution.

When using low frame rates, we observed blurring artifacts in the world images when fast head movements were performed. These effects were alleviated with  $f > 30$  fps. Thus, if images

<sup>1</sup><https://github.com/JirongZhang/DeepHomography>



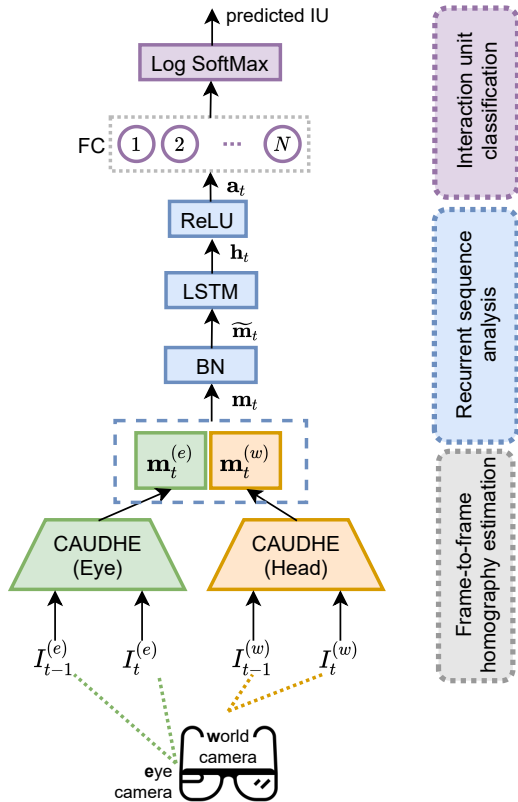


Figure 1: Proposed architecture for head and eye gesture recognition. If only head gestures are considered, only the head CAUDHE instance is required, and no concatenation of the world and eye output features is needed.

Table 2: Final configuration of acquisition (A) and working (W) resolutions after subsampling

Camera	Image size, $w \times h$ (px)		frame rate (fps)	
	A	W	A	W
World	$640 \times 480$	$192 \times 144$ (30%)	60	Up to 30
Eye	$192 \times 192$	$192 \times 192$ (100%)		

are high quality, homography estimation should improve. However, computational resources impose constraints on both the image size (to prevent memory overflow) and the frame rate (to keep under the limited computational power). Therefore, both spatial and temporal subsampling were required (Table 2), and their effects are discussed below (subsection 3.4).

## 2.4 Inference and online recognition

For efficiency at inference time, the input video frames are fed into CAUDHE in batches of  $K$  frame pairs for processing  $K$  homographies in parallel on the GPU. The  $K$  resulting features ( $\mathbf{m}_t$ ) are reshaped and fed to the LSTM as a  $K$ -length sequence. Although predictions of IUs are performed frame-wise, for more robust classification, majority voting is applied to the resulting  $K$  predicted IU labels. Here,  $K = 10$  was chosen as a good tradeoff between computational efficiency and classification delay.

Table 3: Distribution of instances of IUs in the dataset

IU	Length (s)	%	# instances
Neutral	423.77	70.63	N/A
ShakingHead	37.38	6.23	25
NoddingHead	34.73	5.79	26
ComeHere	27.13	4.52	30
Maybe	46.74	7.79	30
Surprise	30.25	5.04	32

## 3 EXPERIMENTS

### 3.1 Configuration

For the purposes of this work, the images from the world camera and from the right-eye camera of the Pupil Core headset [12] were used.

To the best of our knowledge, no public egocentric gesture dataset exists that meets the required criteria (subsection 2.1). Therefore, we collected a dataset with 10 minutes of video, half indoors (close-to-camera walls and objects) and half outdoors (distant background), with about 150 seconds (10 videos  $\times$  15 seconds/video) from each of four participants<sup>2</sup>. Each of the 40 videos (10 videos per participant) contains 3–4 non-overlapping repetitions of a single non-neutral IU. The IU statistics are summarized in Table 3. Video frames were annotated with the corresponding true IU for supervised learning. Since **Surprise** turned out to be a particularly subtle IU, it is separately studied within subsection 3.3, while the rest of the reported results consider the other five IUs.

To account for the stochastic nature of training neural models, 30 repetitions were performed, over which performance statistics on the validation sets are reported. Experiments were run on modest low-cost hardware (PC, 8 GB, 1.8 GHz, GeForce MX250 with 2 GB GPU). Most software was developed using the Python ecosystem (NumPy, pandas, scikit-learn, PyTorch, etc.).

The model was trained for 30 epochs, with Adam optimizer, a learning rate of  $5 \cdot 10^{-4}$ , weight decay penalty of  $10^{-2}$ ,  $\beta_1 = 0.9$ ,  $\beta_2 = 0.999$ , and PyTorch’s *ReduceLROnPlateau* scheduler. A stratified, IU label-based split of 75% of training instances was used, except in subsection 3.5.

### 3.2 Homography vs. deep features

For gesture recognition, an obvious first choice is to use the 8 values of the estimated homography as input to the LSTM ( $\mathbf{m}_t$  in Figure 1). However, we are not concerned on motion estimation itself, but on a qualitative representation of motion that can properly characterize the different interaction units. Therefore, we hypothesized that using the output of a hidden layer of CAUDHE could be beneficial. In particular, the output of the last 2D average pooling layer of CAUDHE (512 features) was used as deep features, and compared with the 8-dim homography values. As found by the distribution of the maximum accuracy (Figure 2), using the deep features for  $\mathbf{m}_t$  turns out to be favorable, which indicates that this qualitative

<sup>2</sup>This work has been approved by the deontological board of Universitat Jaume I (file code “CD/70/2021”, date June 17th, 2021). Human subjects participated after their informed consent.



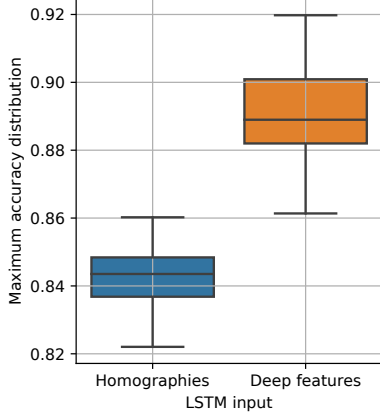


Figure 2: Maximum accuracy with different motion representations used as input to the LSTM

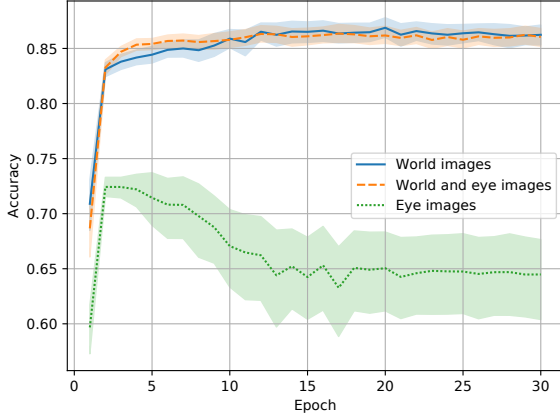


Figure 3: Average accuracy with world and/or eye images

representation of motion is richer and more discriminative than the homography estimates. Similar results were obtained for other performance metrics (precision, recall, and  $F_1$  score).

### 3.3 Using the world and/or eye images

We evaluated how the world ( $I_t^{(w)}$ ) and eye ( $I_t^{(e)}$ ) images contribute to the recognition performance. It can be observed (Figure 3) that the performance is very poor when only eye images are considered, which is not surprising given that the interaction units are heavily head-based. Although the joint consideration of the world and eye images does not improve performance, it is interesting that the recognition does not degrade even when eye images do not bring clearly distinctive information. This is a promising indication that the model might leverage on eye images for capturing commonalities and individual differences for a larger set of images from more participants and repetitions, or when more interaction units, some relying more on eye cues (blinks, winks, subtle motions, etc.), are considered. As an illustrative example, the recognition of the Surprise IU benefits significantly from including the eye images, with an  $F_1$  score about twice that of using the world images only (Figure 4).

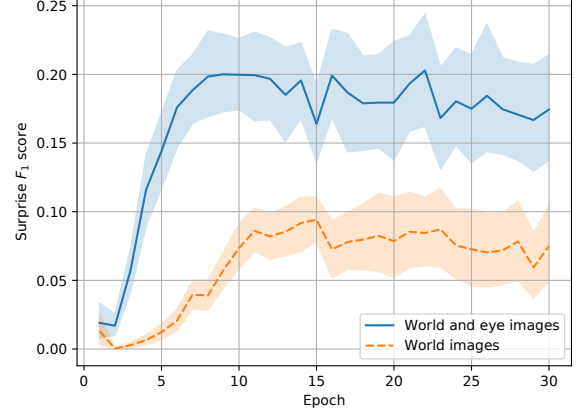


Figure 4: Average  $F_1$  for Surprise with and without eye images

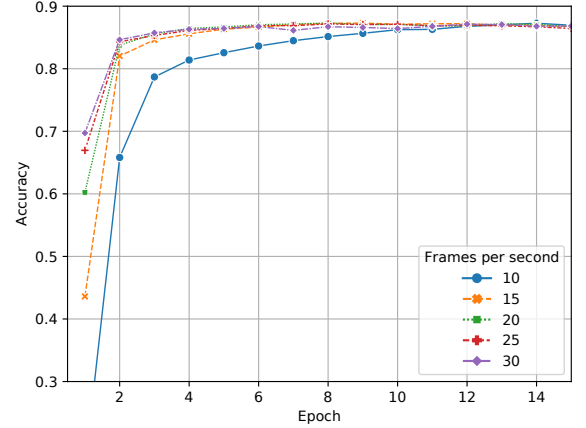


Figure 5: Average accuracy with different frame rates

### 3.4 Effect of subsampling

Regarding spatial subsampling, it was observed that  $192 \times 144$  (30% of the original VGA resolution) worked well in most scenarios. For temporal subsampling, the analysis of the network convergence with different frame rates (Figure 5) reveals that, although all get to approximately the same recognition accuracy, convergence is faster with higher frame rates. For instance, for  $f = 10$  fps, more than 10 epochs are required to get an accuracy which is obtained with 5 or less epochs for the other frame rates. The likely reason for this behavior is that the baseline between two consecutive frames is smaller with higher frame rates, and this benefits the homography estimation network. Furthermore, the robustness against smaller frame rates can be attributed to the use of deep features. For the final version of the proposed system,  $f = 20$  fps is chosen as a good tradeoff solution.

### 3.5 Generalization ability

To evaluate the ability of the proposed model to recognize IUs performed by different subjects (authors) or against different backgrounds (places), we compare the stratified dataset split to the author-based splits (i.e. leaving-one-author out), and place-based splits (i.e. indoor and outdoor recordings are separately considered in the training and test splits). Results (Figure 6) indicate that in the author-based case the maxi-



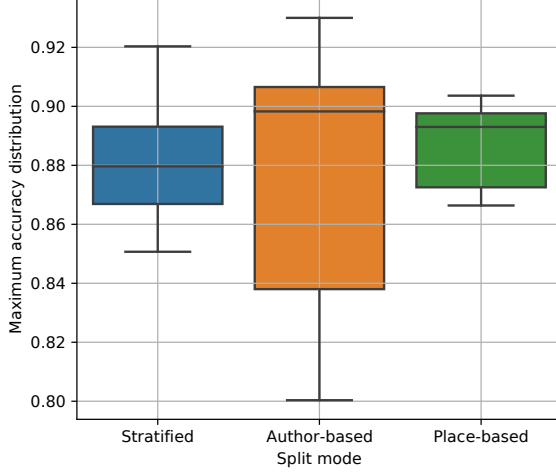


Figure 6: Distribution of the maximum accuracy on validation videos during training, for different dataset split methods

maximum accuracy has larger variability than in the stratified case, since different subjects perform the gestures differently, but in most training repetitions the maximum accuracy was nonetheless high (about 84%). Regarding the place-based split, the performance metric has lower variability and similar or better average value than the stratified case, which is a good sign of the ability of CAUDHE to deal with scenes with backgrounds at different depths, and possibly the positive effect of using deep features. Furthermore, being motion-based, the recognition approach is not biased by the different backgrounds, which might be distracting with appearance-based approaches. Taken these results together, and given the limited data available, it can be argued that the model generalizes reasonably well to different scenes and users.

### 3.6 Overall performance

To understand which IUs are generally better recognized, or with which other IUs they can be misrecognized, it is useful to analyze the confusion matrix (Figure 7). It is revealed that **Neutral** is recognized well by our model. **Maybe** is recognized with a high accuracy, and is the best recognized “non-neutral” IU. **ShakingHead** is recognized fine as well, but is confused sometimes with **Neutral**. Finally, **NoddingHead** and **ComeHere** can also be mistaken, as they both imply vertical head movements, and their difference is somehow subtle and hard to distinguish. As the **ComeHere** movements are more subtle, it is more frequently confused with **Neutral**.

### 3.7 Online prediction

Finally, in addition to global performance metrics, it is insightful to see the predicted IUs over time. Results (Figure 8) indicate that **ShakingHead** (Figure 8a) and **Maybe** (Figure 8d) are generally the best recognized interaction units, and the model tends to label incorrectly only the frames close to transitions. **NoddingHead** (Figure 8b) is confused with **ComeHere** and even **Maybe**, but the recognition performance is still acceptable. In the case of **ComeHere** (Figure 8c), although the overall accuracy is low (actions are often misrecognized as **NoddingHead**),

		True IU				
		Ne	Sh	Nh	Ch	Mb
Predicted IU	Ne	2122 <b>96%</b>	31 <b>16%</b>	12 <b>7%</b>	34 <b>25%</b>	14 <b>7%</b>
	Sh	11 <b>0%</b>	158 <b>84%</b>	0 <b>0%</b>	0 <b>0%</b>	0 <b>0%</b>
	Nh	46 <b>2%</b>	0 <b>0%</b>	136 <b>82%</b>	30 <b>22%</b>	2 <b>1%</b>
	Ch	5 <b>0%</b>	0 <b>0%</b>	9 <b>5%</b>	72 <b>53%</b>	0 <b>0%</b>
	Mb	18 <b>1%</b>	0 <b>0%</b>	8 <b>5%</b>	0 <b>0%</b>	192 <b>92%</b>

Figure 7: Confusion matrix. Ne=Neutral, Sh=ShakingHead, Nh=NoddingHead, Ch=ComeHere, Mb=Maybe

the correct IU is detected on the onset of the IU, which is the most important part in practical situations. A video demonstration is given in folder ‘online’ in the Supplementary material.

## 4 DISCUSSION

The proposed approach for egocentric motion-based gesture recognition has been proven reliable in the collected dataset. Further work would be required to test the system with more interaction units and more data. At collection time, some IUs (**NoddingHead** and **ShakingHead**) simply required some prompts from the experimenter to ensure natural performance, but some other IUs required some hints (to avoid “shrugging shoulders” for **Maybe**, since that would not involve head or eyes), or suggestions for some exaggeration (**Surprise** was too subtle otherwise). In the future, elicitation studies might help waive such indications for more natural performance. Another possible extension would be exploring fusion techniques other than feature concatenation for combining world and eye images. Possibly, an alternative, local encoding of eye images (e.g. optic-flow based) would be preferable over the current global motion assumption. An open interesting question is whether performance can be improved if the homography estimation network is trained or fine-tuned with problem-related sequences instead of using the available pretrained weights. Although the human-egocentric perspective is promising and potentially useful in some practical scenarios, this view can be complemented with robot-egocentric and scene-centric visual sensors (e.g. for face, upper-body or full-body analysis), thus aiming at more robust recognition and wider applicability.

## 5 CONCLUSIONS

A motion-based head and eye gesture recognition framework has been proposed that leverages on egocentric visual data from an eyewear device. The approach relies on the combination of an homography estimation convolutional neural network for frame-to-frame motion characterization, and a long short-term memory for capturing longer-range visual depen-



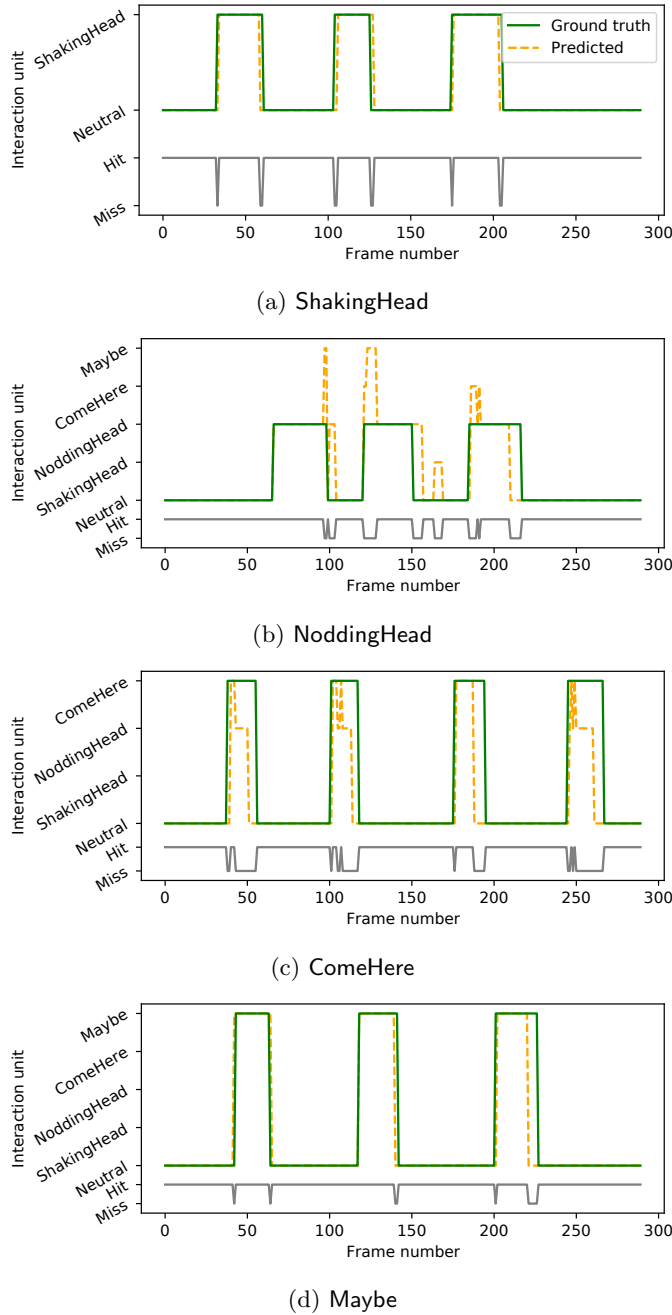


Figure 8: Time diagrams of some validation videos involving various IUs. The bottom gray line helps to appreciate correct recognitions (“hit”) and misrecognitions (“miss”)

dencies. Five general-purpose interaction units have been shown to be recognized with an overall accuracy of over 90% while the system can run in real time with commodity hardware. Moreover, the system performs equally well in a range of frame rates (e.g. 20–30 fps). These are very encouraging results for practical human-robot interaction requirements. One of the most interesting findings is that using the output of a hidden layer of the homography network increases the recognition performance over using the actual output of raw homography values.

## ACKNOWLEDGMENT

We are grateful to the participants in the video capture sessions.

## References

- [1] M. Avdic, N. Marquardt, Y. Rogers, and J. Vermeulen. Machine body language: Expressing a smart speaker’s activity with intelligible physical motion. In *Designing Interactive Systems*, 2021.
- [2] C. Breazeal, C. Kidd, A. Thomaz, G. Hoffman, and M. Berlin. Effects of nonverbal communication on efficiency and robustness in human-robot teamwork. In *IROS*, 2005.
- [3] F. Carrara, P. Elias, J. Sedmidubsky, and P. Zezula. LSTM-based real-time action detection and prediction in human motion streams. *Multimedia Tools and Applications*, 78(19), Oct. 2019.
- [4] H. Cochet and J. Vauclair. Deictic gestures and symbolic gestures produced by adults in an experimental context: Hand shapes and hand preferences. *Laterality*, 19(3), 2014.
- [5] H. Drewes, A. De Luca, and A. Schmidt. Eye-gaze interaction for mobile phones. In *Mobility*, 2007.
- [6] T. Feix, J. Romero, H.-B. Schmiedmayer, A. M. Dollar, and D. Kragic. The GRASP taxonomy of human grasp types. *IEEE Trans. on Human-Machine Systems*, 46(1), 2016.
- [7] K. Fujii, G. Gras, A. Salerno, and G.-Z. Yang. Gaze gesture based human robot interaction for laparoscopic surgery. *Medical Image Analysis*, 44, 2018.
- [8] S. Hueber, C. Cherek, P. Wacker, J. Borchers, and S. Voelker. Headbang: Using head gestures to trigger discrete actions on mobile devices. In *Intl. Conf. on Human-Computer Interaction with Mobile Devices and Services*, 2020.
- [9] C. T. Ishi, D. Machiyashiki, R. Mikata, and H. Ishiguro. A speech-driven hand gesture generation method and evaluation in android robots. *IEEE Robotics and Automation Letters*, 3(4), 2018.



- [10] M. M. Islam and T. Iqbal. Multi-GAT: A graphical attention-based hierarchical multimodal representation learning approach for human activity recognition. *IEEE Robotics and Automation Letters*, 6(2), 2021.
- [11] Y. Ji, Y. Yang, F. Shen, H. T. Shen, and X. Li. A survey of human action analysis in HRI applications. *IEEE Trans. on Circuits and Systems for Video Technology*, 30(7), July 2020.
- [12] M. Kassner, W. Patera, and A. Bulling. Pupil: An open source platform for pervasive eye tracking and mobile gaze-based interaction. In *Adjunct Proc. of the ACM Intl. Joint Conf. on Pervasive and Ubiquitous Computing*, 2014.
- [13] D. Kim, B. B. Kang, K. B. Kim, H. Choi, J. Ha, K.-J. Cho, and S. Jo. Eyes are faster than hands: A soft wearable robot learns user intention from the egocentric view. *Science Robotics*, 4(26), 2019.
- [14] M. Kutbi, X. Du, Y. Chang, B. Sun, N. Agadakos, H. Li, G. Hua, and P. Mordohai. Usability studies of an egocentric vision-based robotic wheelchair. *Journal of Human-Robot Interaction*, 10(1), July 2020.
- [15] Y. Li, C. Lan, J. Xing, W. Zeng, C. Yuan, and J. Liu. Online human action detection using joint classification-regression recurrent neural networks. In *ECCV*, 2016.
- [16] C. Liu, C. T. Ishi, H. Ishiguro, and N. Hagita. Generation of nodding, head tilting and eye gazing for human-robot dialogue interaction. In *ACM/IEEE Intl. Conf. on Human-Robot Interaction*, 2012.
- [17] C. Matuszek, L. Bo, L. Zettlemoyer, and D. Fox. Learning from unscripted deictic gesture and language for human-robot interactions. *Proc. of the AAAI Conf. on Artificial Intell.*, 28(1), June 2014.
- [18] T. Nguyen, S. W. Chen, S. S. Shivakumar, C. J. Taylor, and V. Kumar. Unsupervised deep homography: A fast and robust homography estimation model. *IEEE Robotics and Automation Letters*, 3(3), 2018.
- [19] T. Nukarinen, J. Kangas, O. Špakov, P. Isokoski, D. Akkil, J. Rantala, and R. Raisamo. Evaluation of HeadTurn: An interaction technique using the gaze and head turns. In *NordiCHI*, 2016.
- [20] J. Ondras, O. Celiktutan, P. Bremner, and H. Gunes. Audio-driven robot upper-body motion synthesis. *IEEE Trans. on Cybernetics*, 2020.
- [21] J. R. Searle. A taxonomy of illocutionary acts. In *Language, Mind and Knowledge*. University of Minnesota Press, 1975.
- [22] S. Song, C. Lan, J. Xing, W. Zeng, and J. Liu. Spatio-temporal attention-based LSTM networks for 3D action recognition and detection. *IEEE Trans. on Image Processing*, 27(7), 2018.
- [23] C. Stahl, D. Anastasiou, and T. Latour. Social telepresence robots: The role of gesture for collaboration over a distance. In *Proc. of the 11th Pervasive Tech. Related to Assistive Env. Conf.*, 2018.
- [24] J. Stolzenwald and W. W. Mayol-Cuevas. Rebellion and obedience: The effects of intention prediction in cooperative handheld robots. In *IROS*, 2019.
- [25] Y. Terzioğlu, B. Mutlu, and E. Şahin. Designing social cues for collaborative robots: The role of gaze and breathing in human-robot collaboration. In *ACM/IEEE Intl. Conf. on Human-Robot Interaction*, 2020.
- [26] O. Špakov, P. Isokoski, and P. Majaranta. Look and lean: Accurate head-assisted eye pointing. In *Proc. of the Symposium on Eye Tracking Research and Applications (ETRA)*, 2014.
- [27] O. Špakov and P. Majaranta. Enhanced gaze interaction using simple head gestures. In *ACM Conf. on Ubiquitous Computing (UbiComp)*, 2012.
- [28] J. Zhang, C. Wang, S. Liu, L. Jia, N. Ye, J. Wang, J. Zhou, and J. Sun. Content-aware unsupervised deep homography estimation. In *ECCV*, 2020.
- [29] J. Zhang, L. Zhuang, Y. Wang, Y. Zhou, Y. Meng, and G. Hua. An egocentric vision based assistive co-robot. In *IEEE Intl. Conf. on Rehabilitation Robotics (ICORR)*, 2013.